1

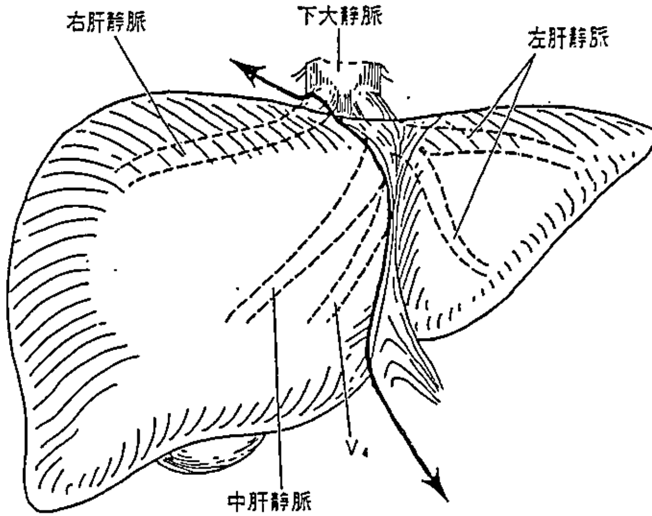

図1　肝右3区域切除術の概念
肝円索および肝鎌状間膜を結ぶ線（面）より右側に位置する3区域を切除する術式であり，中肝静脈を左肝静脈との合流部で，右肝静脈を下大静脈への流入部で切離することになる。概念上は尾状葉切除はこの術式に含まれないが，われわれは右側尾状葉を同時に切除している。肝門部胆管癌の場合にはSpiegel部も切除範囲に含める

2

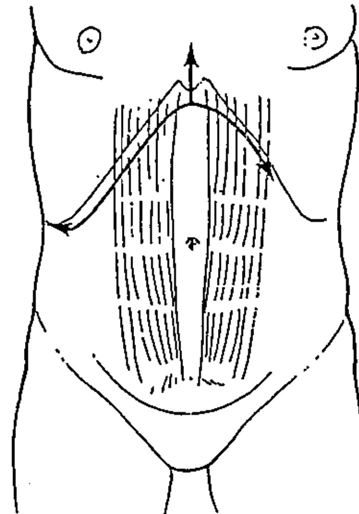

図2　皮膚切開
患者の体位は仰臥位とし，逆T字切開にて開腹。左縁は腹直筋外縁から，右縁は右腋窩線までを，上縁は剣状突起部までを目安とする。右の側腹部では，皮膚切開線をやや頭側に切り上げるように置く。施設によっては開胸・開腹・横隔膜切開を薦めるところもあるが，われわれは図3の開創鉤を使用することで開腹アプローチのみで通常十分な術野を得ている

3

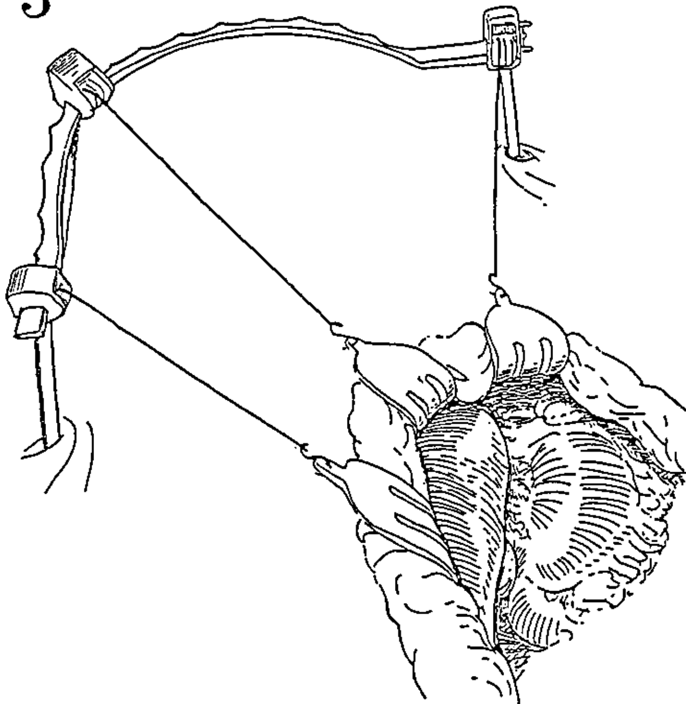

図3　肋弓下を大きく開くための牽引鉤とアーチ（ケント牽引開創器™）
皮膚と腹膜を縫着して創面を保護した後，四枚ガーゼで保護して，両側または3方から鉤をワイヤーで牽引する。上方のアーチは清潔範囲内にあるので，牽引する方向を自在に調整できる

4

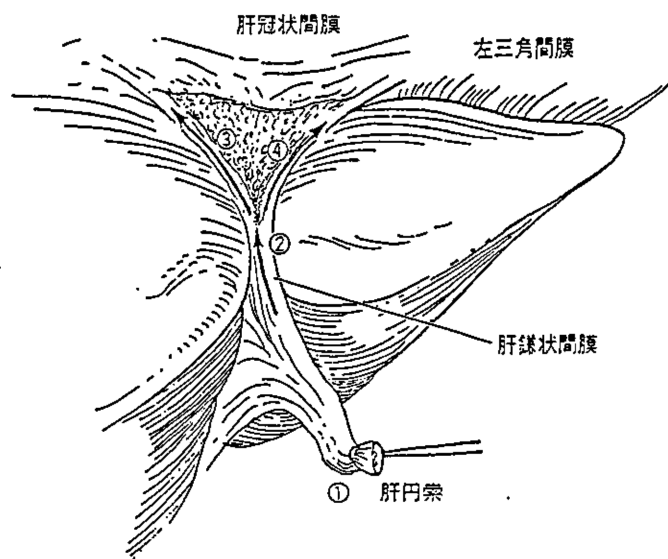

図4　肝鎌状間膜の切離と bare area 漿膜の切開

開腹操作の横切開時に肝円索を切離するが，このときの結紮糸は後の牽引糸として残しておく。肝鎌状間膜を②のように，bare area に向かってしだいに肝表面に近くなるように切離する。その後，肝鎌状間膜を形成していた漿膜は左右に分かれて肝冠状間膜となり，その間に bare area を構成するため，③④のように切離を進めながら bare area を剥離する。続いて右三角間膜を肝実質に接して切離を進め，後ほど肝右葉脱転時に右側方から進めてくる切離ラインと続けられるようにしておく。通常，下横隔静脈は温存できるが，その損傷が危ぶまれるときにはこれを結紮切離してもよい

5

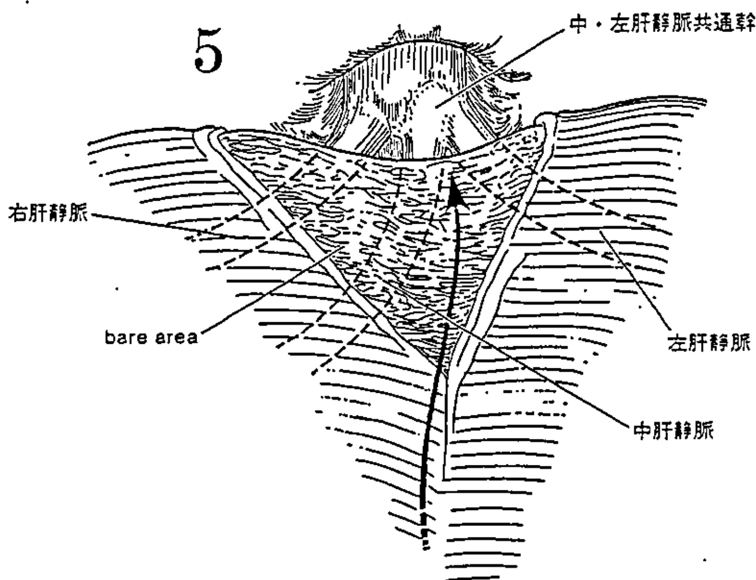

図5　肝静脈の露出

下大静脈の前面に向かって bare area の剥離を慎重に進めると，左・中肝静脈の共通幹と右肝静脈の根部が露出される。共通幹の根部を肝実質側に優しく押さえてゆくようにすると多くの場合，左肝静脈と中肝静脈の合流部が小さな窪みとして認識できるようになり，肝実質切離線の上端を決定できる

6

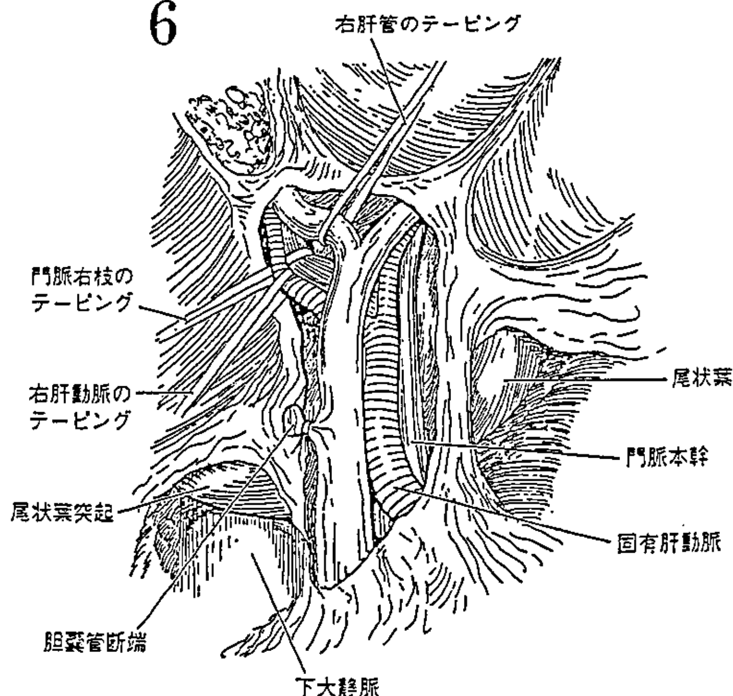

図6　肝門部の整理：肝動脈・右肝管の処理

肝十二指腸間膜を開き，胆嚢管・胆嚢動脈を結紮切離する。胆嚢は原理上摘出する必要はなく，右葉とともに切除することになる。しかし，胆嚢癌などでなく，胆摘を行うことが oncology の観点から根治性を失う原因にならない場合には，胆摘を行ったほうが肝門部の術野を展開するうえで有利である。総胆管の後方をクロスしてその右側に出てくる右肝動脈を求め，これより右肝動脈と中肝動脈の根部を同定し，これらを結紮切離する。これにより固有肝動脈から左肝動脈を肝十二指腸間膜の左側に寄せ分離することができる

左右肝管の分岐部が簡単に同定される場合には，右肝管を結紮切離する。左右の分岐部が肝門板の厚い Glisson 被膜で同定しにくい場合には，肝実質切離を先行させ，切離が肝門板に至ってから鋭的に右肝管を切離するほうが安全である。無理に右肝管を剥離しようとすると，温存すべき左枝を傷つける場合があり注意を要する

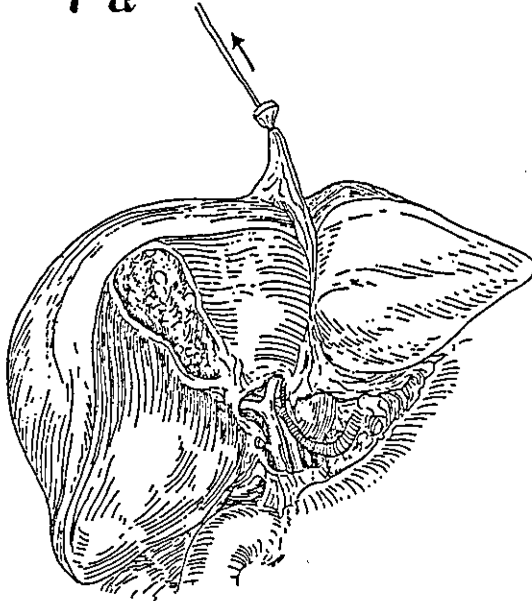

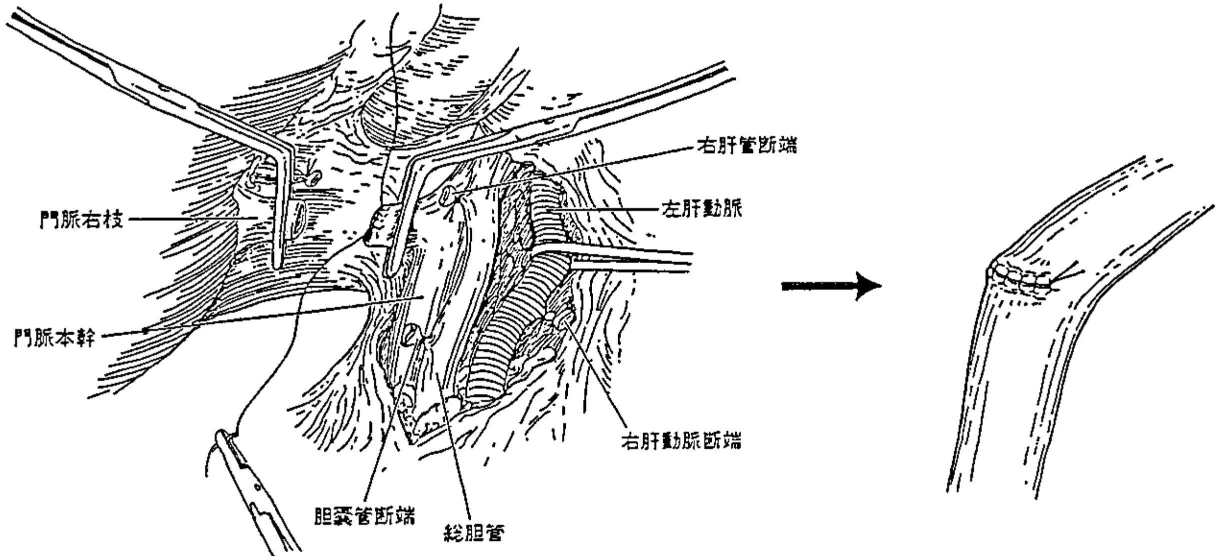

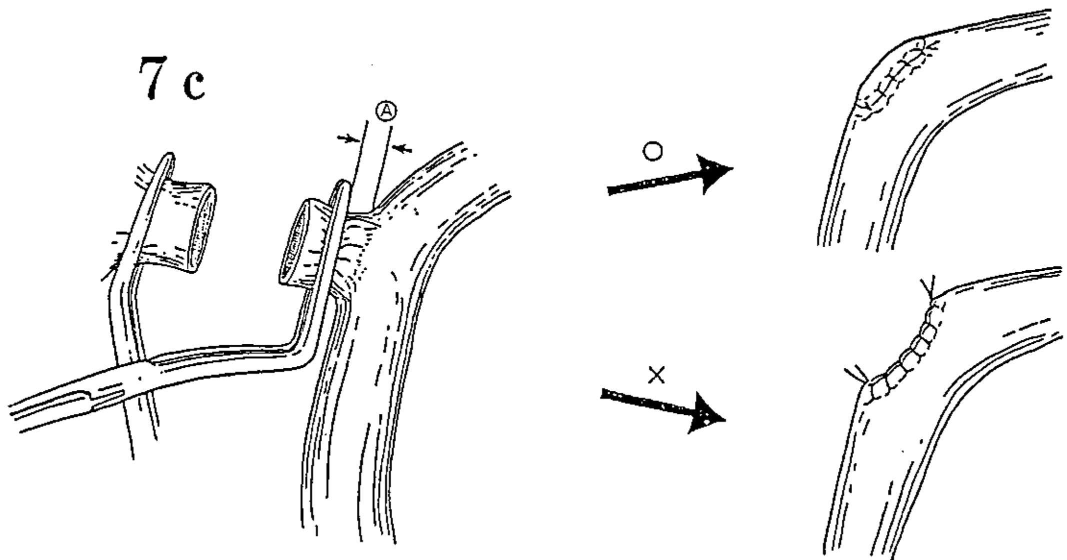

図7　肝門部の整理：門脈右枝の処理

門脈は肝十二指腸間膜で包まれているが，間膜の右側より総胆管の背側を剥離すると容易にその本幹を同定できる。それより門脈右枝を求め，テーピングを行った後に離断する。門脈右枝の encircle の際に門脈から右尾状葉に出る枝に注意し，必要があればこれを結紮切離する。門脈右枝の根部を剥離する際には，助手に肝円索にかけた牽引糸を強く上方に引かせると肝門部の視野が広く展開される(a)。離断の際に血管鉗子をかける方向を b のように門脈本幹の軸と直角方向（anteroposteriorly）にかけておくと，縫合閉鎖線が横縫いの状態となり，門脈を狭窄させる心配がない。c のように門脈本幹の軸と平行に処理しても通常問題はないが，その場合，図中Ⓐの距離を調整してとらないと管径を狭窄させることになるので注意する。門脈に腫瘍栓が存在する場合にはこの時点で，門脈本幹，左右門脈枝を別々にテーピングし，出血をコントロールできるようにしておいてから腫瘍栓を摘出する

8

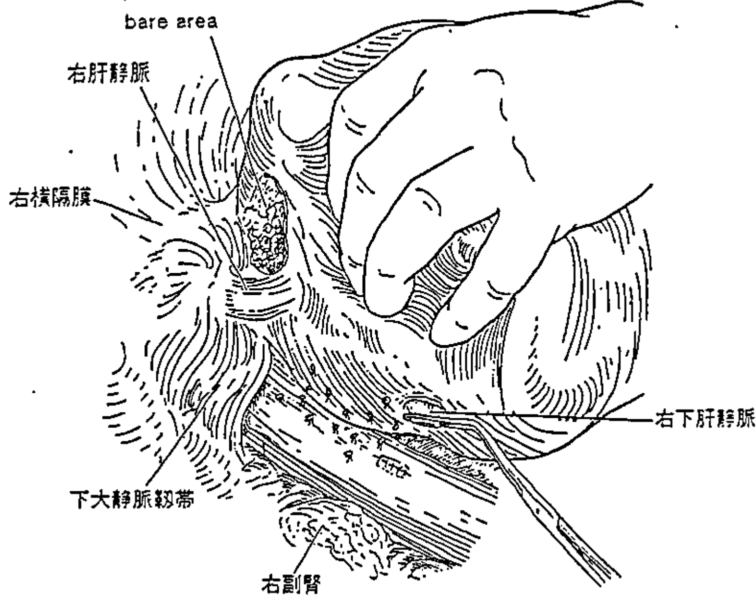

図8　右葉の授動と脱転

肝右葉の授動は肝門部処理が終わってから行うと，右葉の体積がいくぶん小さくなってやりやすい。肝下縁に沿って肝腎間膜を切離し，下大静脈の右縁に出る。続いて頭側に向かって後腹膜より翻転して，肝被膜に至る漿膜を切離しつつ，疎な結合織の層で剥離を進め，頭側からの右三角間膜の剥離部に合流する。この際，右副腎が黄金色の組織として現れてくるので，組織内に切り込んで出血させないように，慎重にかつ完全に後腹膜側に落とし込む

徐々に肝を左側・頭側に脱転しながら剥離を進めると，下大静脈の右側から前面に何本もの短肝静脈が現れるので，これらを順次結紮切離する。剥離は下大静脈の正中を越えて，右尾状葉を完全に下大静脈より遊離する。とくに，右下肝静脈と呼ばれる太い短肝静脈は結紮がはずれると大出血となるので，血管鉗子で挟み，切離後プロリン5-0糸にて縫合閉鎖する

さらに頭側に剥離を進めていくと，右肝静脈根部を覆う硬い下大静脈靱帯が現れる。右肝静脈を損傷しないように注意しながら，この靱帯を切離すれば肝右葉の脱転は終了する。ここで，右肝静脈を処理することも可能であるが，無理にこの時点で encircle などの処理をしなくても，肝実質切離を終了すると最後に安全に切離できる

9

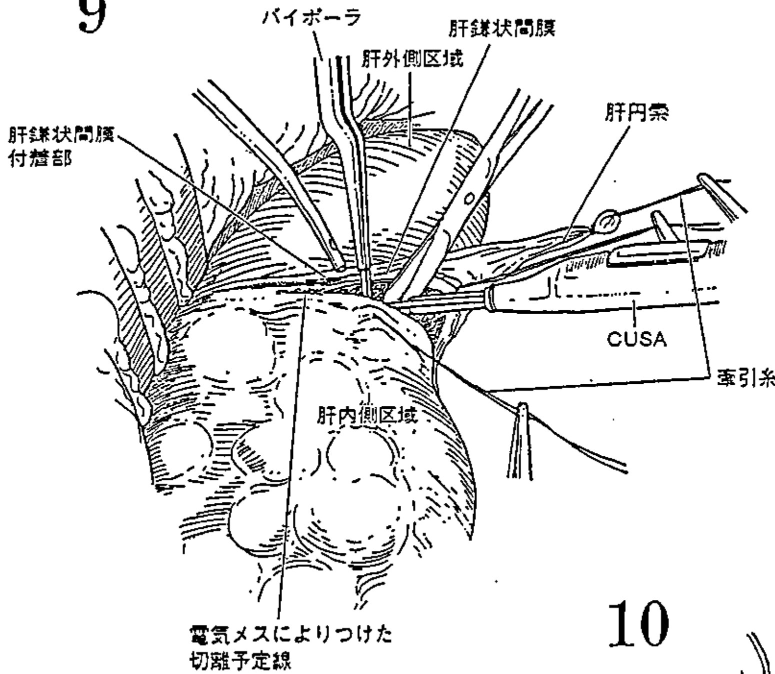

図9　肝実質の切離

肝実質切離線は肝鎌状間膜の右側縁に沿って矢状線に一致する。実質切離を CUSA と水流滴下式のバイポーラで，前方より後方に向かって進める。切離予定線の両サイドにプロリン3-0糸にて牽引糸をかけ，助手には左側の牽引糸と肝円索にかけた牽引糸を一緒にして尾側に引かせ，右側の牽引糸を自分で引くことで切離面の展開を調整する

10

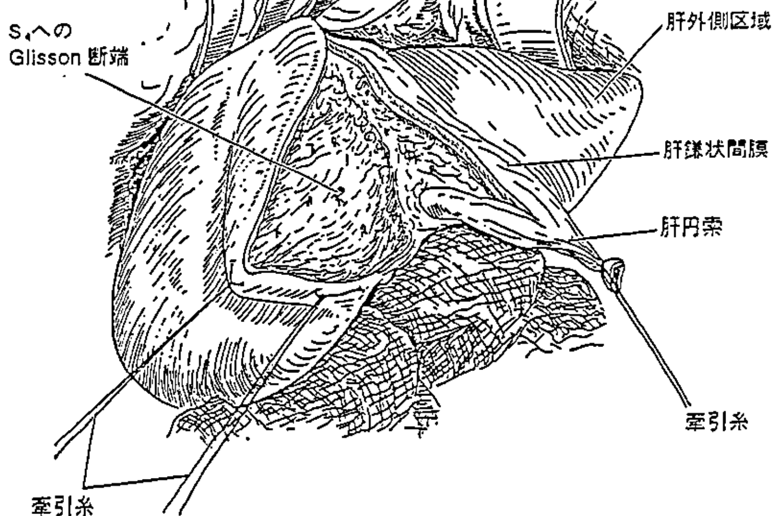

図10　肝実質切離の方向

切離面は左葉の内側区域と外側区域の境界面に相当し，内側区域へ向かう数本の Glisson 系脈管と中肝静脈根部以外には重要な構造物は現れない。太い Glisson は残肝側を結紮し，切除側をヘモクリップで処理して切離する。細い Glisson と肝静脈系脈管は，バイポーラで焼灼のうえ切離する。肝門部処理の際に右肝管を処理していない場合には，実質切離が肝門板に達したところで左枝を傷つけないように注意しつつ鋭的に切離し，断端をプロリン6-0糸にて胆汁漏を生じないようにていねいに縫合閉鎖する

11a

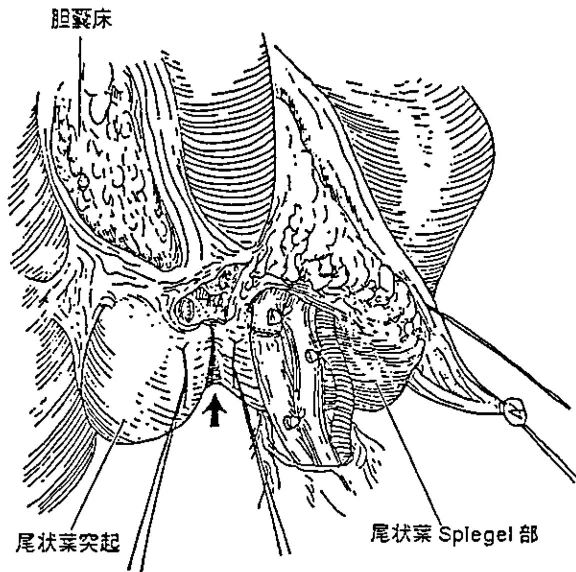

11b

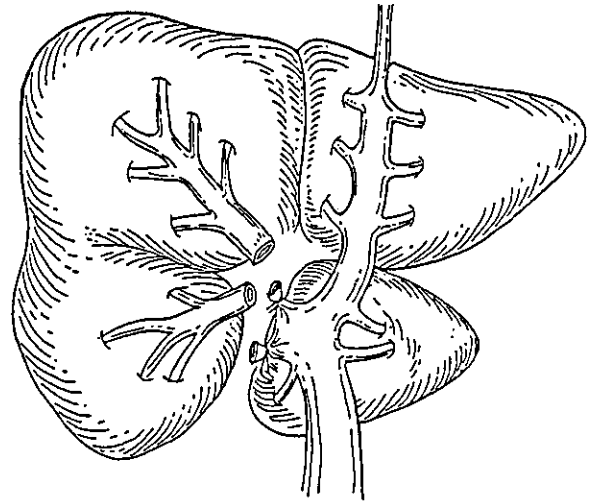

図11　尾状葉の切離
われわれは門脈右枝を分岐部根部で処理しているため右側尾状葉を合併切除しているが，こうすると下大静脈前面に至るまでまっすぐ矢状面で貫くのみでよい。この場合，尾状葉の Spiegel 部右端にあたるくびれの部分より切離を加え，先の実質切離面と連続させる。全尾状葉を温存する場合には肝門部 Glisson 処理の際に，左右分岐部で処理をせずに b のように右 Glisson の前後枝の分岐部で処理し，右尾状葉を支配する枝を温存しておく

12

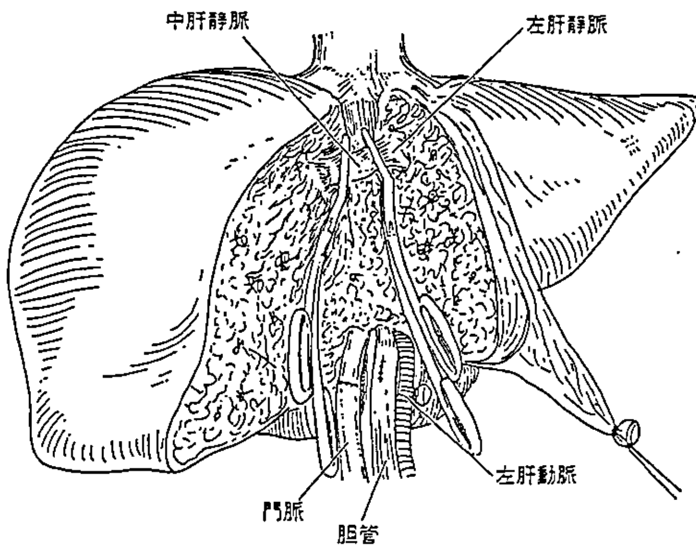

図12　中肝静脈の処理
実質切離が頭側に進み，bare area の直下に近づくと中肝静脈と左肝静脈に流入する肝静脈の枝がそれぞれの本幹に近くなる。引き抜くと出血のコントロールがしにくくなるので，傷つけないように慎重に切離を進める。切離の方向を図5で確認しておいた中肝静脈根部の真上に向かうようにしてゆくと，切離面に中肝静脈の左側壁が現れ，続いて左肝静脈根部との合流部の股の部分に至る。この部で中肝静脈前面の実質組織を CUSA で破砕吸引すると根部が完全に露出され，下大静脈前面までが開放される。中肝静脈根部背側の組織を CUSA でていねいに吸引し，テーピングのうえ，血管鉗子で挟んで切離する。断端はプロリン5-0糸にて縫合閉鎖する

13

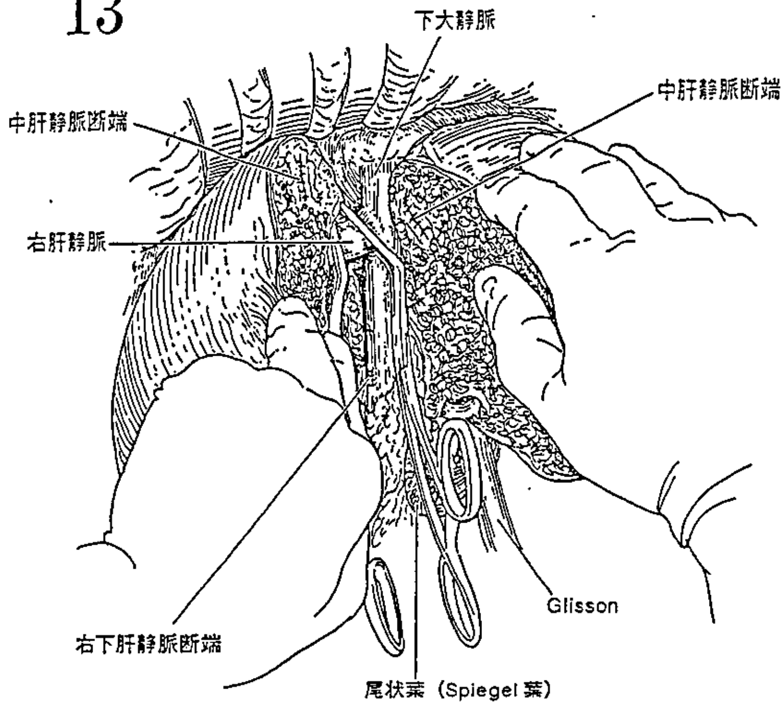

図13　右肝静脈の処理
中肝静脈の切離が完了した後，すでに剥離を終えてある下大静脈の前面に左示指を挿入すると，残る組織は尾状葉下大静脈部の薄い実質のみである。これを CUSA で切離後，下大静脈前面の被膜を電気メスで切離すれば，切除肝は右肝静脈でのみつながった状態となる。根部を血管鉗子で挟んで切離，標本を摘出すれば肝右3区域切除が完了する。右肝静脈根部の中枢側断端は，プロリン4-0糸にて縫合閉鎖する

14

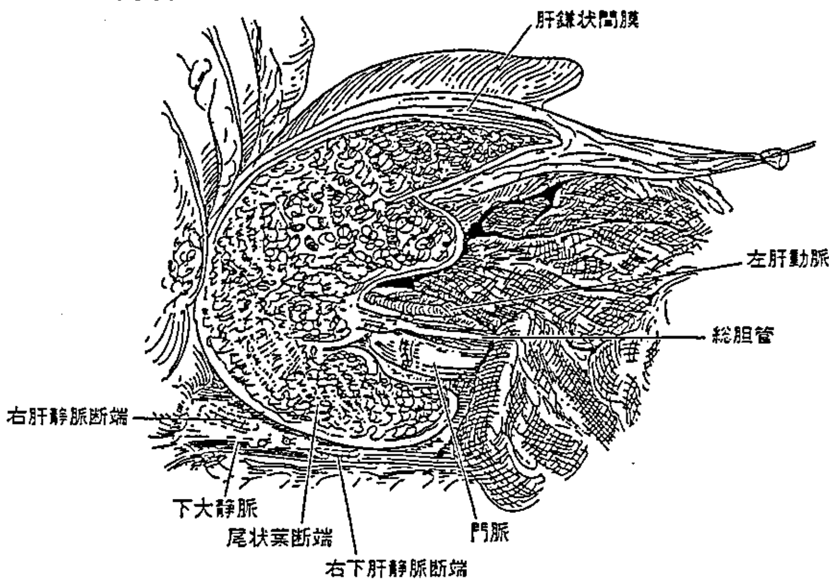

図14　肝右3区域切除完了図
肝切離面は肝鎌状間膜より垂直に，下大静脈前面まで平らに切離されている

15

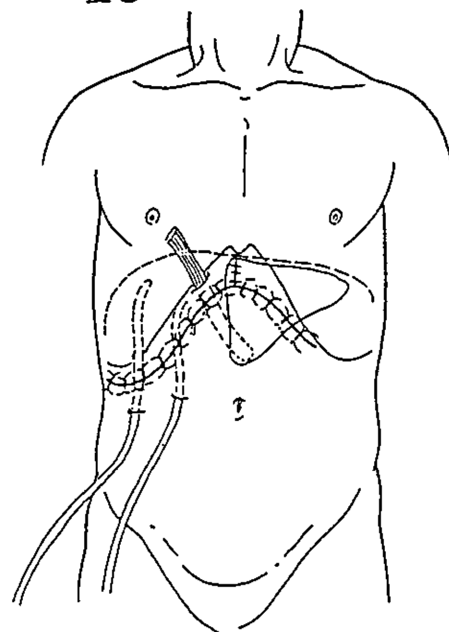

図15　閉腹とドレーンの挿入
肝断面からの出血・胆汁漏のないことを確認したうえで，フィブリン糊をスプレー散布する。胆汁漏が疑われる場合には胆嚢管より術中胆管造影，または色素注入を行い，部位の特定をしたうえで処理を行う。必要な場合には胆嚢管より c-tube を留置して，減圧を図っておくことも工夫である
ドレーンを右横隔膜下と肝切離断面において，腹壁を3層に閉鎖する

尾状葉の全切除を伴う場合

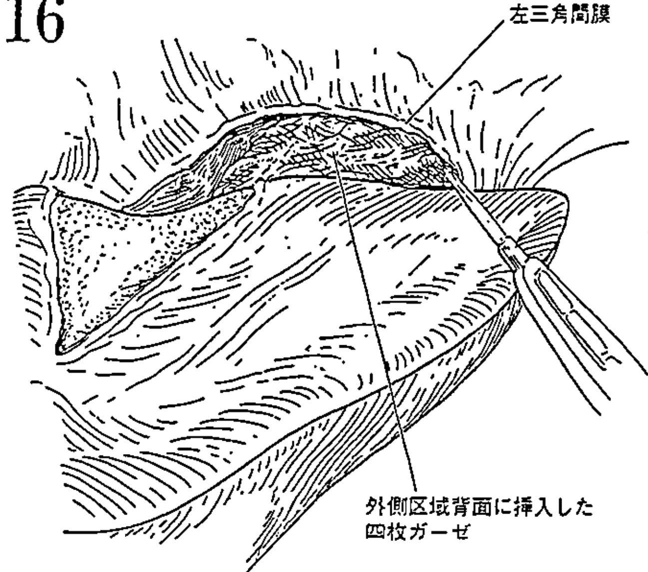

図16　左三角間膜の切離と肝門部処理

尾状葉を全切除する場合には，外側区域と尾状葉 Spiegel 部の間で Arantius 管を切離し，Spiegel 部を下大静脈より剝離する必要がある。このために，図4で肝冠状間膜を切離後，左三角間膜も切離し，外側区域を遊離して右側に脱転できるようにしておく。左三角間膜の切離に先立って，胃と脾臓を右手で背側下方に圧排しながら四枚ガーゼを肝外側区域との間に挿入すると，ガーゼが三角間膜の前面より透見できるため，電気メスで直接三角間膜を切離しても安全である。肝門部の整理の際に，門脈左枝水平部より尾状葉に流入する細い枝が数本あるので，出血させないように注意して結紮切離する。胆管は尾状葉全切除を伴うような症例では通常，左 Glisson 水平部の末梢で切離することになる

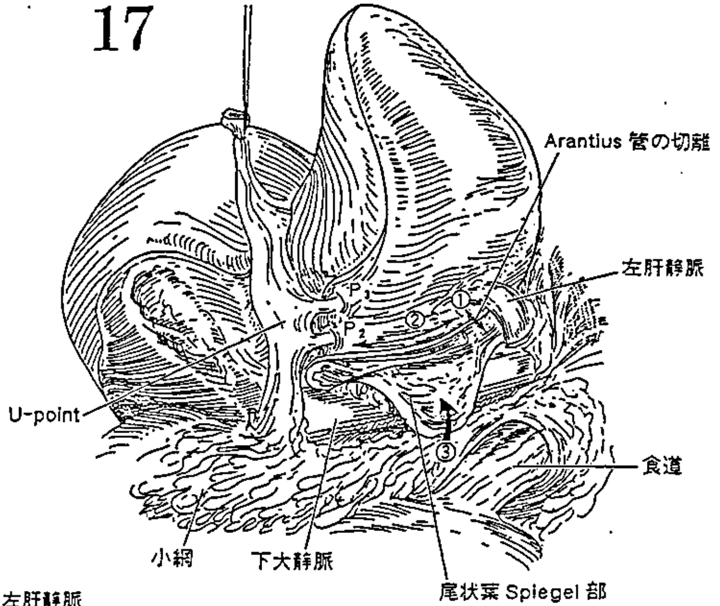

図17　Arantius 管の切離と尾状葉 Spiegel 部の遊離

肝右葉の授動終了後，外側区域を右方に脱転し，小網を肝付着部近くで切離すると Arantius 管が現れるので，①のようにこれを切離する。次に②のように Arantius 管に沿って，外側区域と尾状葉の間で翻転している漿膜を切離しておく。続いて，後腹膜より尾状葉 Spiegel 部の被膜につながる漿膜を切開して，下大静脈前面と Spiegel 部の間で③のように短肝静脈群を切離しつつ剝離して，図8における剝離層と連続させる

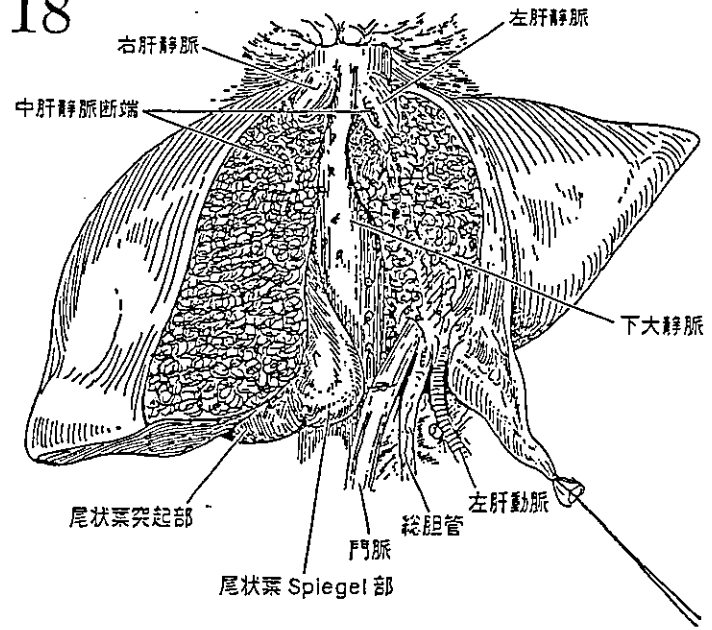

図18　肝実質切離

肝実質切離が尾状葉 Spiegel 部の前面の深さに達し，中肝静脈根部を処理したところで右手の指先を揃えて外側区域の背面と尾状葉の前面の間に挿入し，他方，切離面の底の部分から左方に左手の指先をあてがうと，間に約5 mm ほどの肝実質組織のみを介してお互いに触れ合うことができる。この部分で窓を開けるように交通させると，尾状葉を切除側の肝臓につけた状態で下大静脈の右方に引き出すことができる。あとは図13のように右肝静脈を切離すれば，切除は終了する。左三角間膜を切離した場合には残肝は左肝静脈のみで支えられることになるので，術後に右側の死腔側に rotation をきたして out-flow block をきたす恐れがある。肝鎌状間膜が残っていればそれを閉腹時に横隔膜に固定し，rotation をきたさないようにしておくとよい

肝　臓

ACTA HEPATOLOGICA JAPONICA

第38回　日本肝臓学会総会
講演要旨

会　　長　故　井上恭一
　　　　　関西医科大学第３内科
会長代行　沖田　極
　　　　　日本肝臓学会理事長
会　　期　平成14年６月13日(木)，14日(金)
会　　場　大阪国際会議場

Vol. 43　Supplement (1)

2002

O-105 肝臓外科における JNK 活性化抑制の意義

波多野 悦朗[1]、Bradham Cynthia[2]、上原 徹也[2]、吉田 真規[1]、新田 隆士[1]、原田 信子[1]、小泉 直樹[1]、山本 成尚[1]、Brenner David[2]、山岡 義生[1]
[1]京都大学 医学研究科 消化器外科、[2]ノースカロライナ大学

【目的】安全な肝切除には、虚血再灌流障害、肝再生不全に伴う肝不全に対する対策が必要である。JNK は、虚血再灌流や肝切除により活性化されるが、その役割は、不明である。JNK 特異的阻害剤及び JNK の活性化を抑制するアデノウイルスベクターを用いて以下の実験を行った。

【方法】Wistar rat に可逆的 JNK 特異的阻害剤を前投与し(SPC 群)、1)70%90分肝部分虚血＋30%非虚血葉肝切除後 7 日目の生存率2)60分肝部分虚血後の肝組織像、肝逸脱酵素、caspase-3 活性を vehicle 前処置群と比較した。SD rat を用いて JNK 上流の MAPKKK である TAK1 の dominant-negative form を発現する Ad5dnTAK1 及び c-jun の truncated form である TAM-67を発現する Ad5TAM を肝切除 2 日前に投与し70%肝切除後の3) JNK の活性化を JNK kinase assay 及び phospho-c-Jun の Western blot、c-jun の Northern blot にて、4)肝再生を mitotic index、PCNA index、cyclin E、D、A、B 及び c-myc の Northern blot、Western blot を用いて評価した。

【結果】1)肝切除後 SPC 群の生存率は、vehicle 投与群(27%)に比べ有意に改善(60%)した。2) vehicle 投与群における肝細胞のアポトーシスが、SPC 群で明らかに軽減し、vehicle 投与群に比べ SPC 群では虚血再灌流 6 h 後 ALT が42%低下、caspase-3 活性が、63%低下した。3) PBS もしくは AdLuc 前投与群で肝切除後 JNK の活性化、c-Jun のリン酸化、c-jun の mRNA 発現亢進を認めたが、Ad5dnTAK1 及び Ad5TAM 前投与によりいずれも抑制したが、Ad5dnTAK1 は、NF-κB、p38及び SMAD に無影響であった。4) Ad5dnTAK1 及び Ad5TAM 前投与で肝切除前より PCNA の発現亢進、mitotic index の増加、cyclin 及び c-myc の発現亢進を認めた。

【結論】虚血再灌流障害モデルにおいて JNK 阻害剤によりアポトーシス、肝障害の軽減を認めた。また JNK の活性化抑制は、c-myc の発現を介し肝再生を促した。肝切除の適応拡大における JNK を標的とした "preconditioning" の可能性が示唆された。

O-106 加齢指標蛋白質 SMP30遺伝子破壊によるアポトーシス感受性亢進と臓器変化

丸山 直記[1]、北村 庸雄[2]、榎本 信行[2]、佐藤 信紘[2]
[1]東京都老人総合研究所 分子病理、[2]順天堂大学 医学部 消化器内科

【目的】加齢指標蛋白質 SMP30は肝細胞に多量に発現され加齢と共に発現が減少する蛋白質である。SMP30はカルシウム結合能を持ち299個のアミノ酸からなる他に類似性を持たない蛋白である。SMP30遺伝子は高等動物間で極めて高度の相同性を示し、下等動物にも存在する。SMP30の肝臓における機能を解析するためにSMP30遺伝子を破壊して病態を観察した。

【方法】マウス SMP30遺伝子の第 3 エクソンに Neo遺伝子を挿入することにより SMP30欠損(SMP30-KO)マウスを作製した後、野生型 C57BL/6 マウス(SMP30-WT)に退交配し近交系として確立した。初代肝細胞培養系を用いたアポトーシスの誘導は TNFα とアクチノマイシン D の併用により行い annexinV 染色により測定した。肝臓中の脂質の分析は薄層クロマトグラフィーにより行った。

【成績】SMP30-KO と SMP30-WT 間には生育過程では明らかな変化は認められなかった。SMP30-KO においては TNFα によるアポトーシスの感受性が SMP30-WT に比較して有意に亢進した。抑制系である NFκB の活性化には差が認められなかった。細胞膜カルシウムポンプ活性は SMP30-KO では完全に消失していた。電子顕微鏡による観察では12カ月齢 SMP30-KO 肝臓では脂肪滴の沈着が著明でライソゾームの増加、ミトコンドリアの変性、小胞体の発達が不良、リボソームの減少等が観察された。SMP30-KO マウス肝臓中の脂質成分を薄層クロマトグラフィーで解析した結果、SMP30-WT マウスとの比較では中性脂肪の量的差は無いが、リン脂質あるいはコレステロール量に著明な差異が認められた。過酸化脂質の量は予想に反して SMP30-KO マウスの方が少なかった。

【考案】SMP30-KO マウスにおける TNFα 誘導性アポトーシスに対する感受性亢進はアポトーシス時の細胞内カルシウム上昇にカルシウムポンプが機能しないためと考えられる。ミトコンドリアへのカルシウム移行も同様の機序によるため SMP30-KO マウスではミトコンドリア機能不全が生じている可能性が示唆された。肝臓内脂質成分に著明な差があることは SMP30が脂質代謝に重要な役割を果たしていることが示唆された。

【結語】SMP30はカルシウムポンプを活性化することによりアポトーシス感受性を低下させ、ミトコンドリア機能を保っている。脂質代謝における SMP30の関与が推定された。

ELSEVIER

Journal of Hepatology 41 (2004) 782–789

Journal of Hepatology

www.elsevier.com/locate/jhep

Interferon-αCon1 suppresses proliferation of liver cancer cell lines in vitro and in vivo☆

Toru Hisaka, Hirohisa Yano*, Sachiko Ogasawara, Seiya Momosaki, Naoyo Nishida, Yumi Takemoto, Sakiko Kojiro, Yuno Katafuchi, Masamichi Kojiro

Department of Pathology, Kurume University School of Medicine, Research Center of Innovative Cancer Therapy of the 21 Century COE Program for Medical Science, Kurume University, 67 Asahi-machi, 830-0011 Kurume, Japan

Background/Aims: We investigated the effects of consensus interferon (IFN-αCon1), a nonnaturally occurring type I interferon with higher specific activity than other type I IFNs, on the growth of human liver cancer cells.

Methods: The effect of IFN-αCon1 on the proliferation of 13 liver cancer cell lines was investigated in vitro. Hepatocellular carcinoma (HCC) cells (KIM-1 and HAK-1B) were transplanted subcutaneously into the back of nude mice, then IFN-αCon1 was subcutaneously administered to the mice once a day for 2 weeks, and tumor volume and histology were examined.

Results: IFN-αCon1 expressed a dose-dependent growth inhibitory effect in all cell lines in vitro. KIM-1 tumor volume in mice that received 0.01 μg (10^4 IU)/mouse/day of IFN-αCon1 (similar to the clinical dose for chronic hepatitis C) was 62% of the control, 0.1 μg/mouse/day resulted in 26%, and 1 μg/mouse/day resulted in 10%. HAK-1B tumor volume under the same treatment was 61, 24 and 0% of the control, respectively. The number of apoptotic cells significantly increased and the number of blood vessels significantly decreased with the increase in IFN-αCon1 dose.

Conclusions: IFN-αCon1 suppressed HCC growth in nude mice. These data indicate the potential clinical application of IFN-αCon1 in the prevention and treatment of HCC.

© 2004 European Association for the Study of the Liver. Published by Elsevier B.V. All rights reserved.

Keywords: Angiogenesis; Apoptosis; Antiproliferation; Consensus interferon; Hepatocellular carcinoma; Nude mouse

1. Introduction

Hepatocellular carcinoma (HCC) is one of the most frequently found primary cancers in the world, in particular in Asia and Africa. Many HCC patients have chronic hepatitis or cirrhosis caused by chronic infection of hepatitis B virus (HBV) or hepatitis C virus (HCV) as their background disease [1–3]. Interferon (IFN)-α has been applied in treatment for HBV- and HCV-related chronic hepatitis in several countries because of its suppressive effects on virus replication (reviewed in Ref. [4]). IFN-α possesses high suppressive effects on hepatocellular carcinogenesis [5–7]. Because it possesses not only antivirus effects but also various biological activities such as antiproliferative activity, immunoregulatory activity, anti-telomerase activity, and anti-angiogenesis activity [8,9], IFN-α has been applied in the treatment of malignant diseases including renal cancer and leukemia [4,10].

Antiproliferative effects and the mechanism of actions of IFN-α have been studied in vitro using various human organ-derived neoplastic cells including HCC [11–14], lymphoma, melanoma, and leukemia cells [4,15–26]. We previously reported the relationship between IFN-α receptor expression and antiproliferative effects on 13 liver cancer cell lines [13], i.e. (i) almost all cell lines

Received 10 December 2003; received in revised form 14 May 2004; accepted 2 July 2004; available online 26 July 2004

☆ The authors who have taken part in this study declare that they have no relationship with the manufacturers of the drugs involved either in the past or present and did not receive funding from the manufacturers.

* Corresponding author. Tel.: +81-942-31-7546; fax: +81-942-32-0905.

E-mail address: hiroyano@med.kurume-u.ac.jp (H. Yano).

0168-8278/$30.00 © 2004 European Association for the Study of the Liver. Published by Elsevier B.V. All rights reserved.
doi:10.1016/j.jhep.2004.07.012

express Type I IFN receptor, and (ii) natural human IFN-α arrests cell cycle with or without apoptosis and suppresses cell-proliferation at various degrees. These findings indicate that IFN-α may be an effective remedy with or without other medicines such as anticancer agents.

Consensus interferon, i.e. IFN-αCon1, is a wholly synthetic Type I interferon. The consensus sequence was synthesized through the scanning of several IFN-α non-allelic subtypes and assigning the most frequently observed amino acid in each position [27]. On the molar basis, IFN-αCon1 was more potent in antiviral effects, antiproliferative effects, NK cell activation activity, cytokine induction and IFN-stimulated gene-induction activity than recombinant IFN-αs (e.g. IFN-α2a and IFN-α2b). On the antiviral unit basis, however, those effects and activities were equal in IFN-αCon1 and recombinant IFN-αs [27,28]. These conditions are attributable to the higher affinity of IFN-αCon1 to the array of Type I interferon receptors. This high binding affinity may reflect increased binding capacity and/or signaling at lower protein concentrations [27–29]. With these characteristics, the antitumor effects of IFN-αCon1 to HCC are expected to be more potent than the other IFN-αs, but there have been no in vitro or in vivo studies on the effects.

In the current study, we examined the antitumor effects of IFN-αCon1 on 13 HCC cell lines both in vitro and in vivo, using several concentrations including a low dose that is similar to the level used in clinical application.

2. Materials and methods

2.1. Cell lines and cell culture

This study utilized 11 HCC cell lines (KIM-1, KYN-1, KYN-2, KYN-3, HAK-1A, HAK-1B, HAK-2, HAK-3, HAK-4, HAK-5, and HAK-6), and 2 human combined hepatocellular and cholangiocarcinoma (CHC) cell lines (KMCH-1 and KMCH-2). The cell lines were originally established in our laboratory, and each of the cell lines retains morphological and functional features of original tumor as previously described [13,30–37].

Each cell line was grown in Dulbecco's modified Eagle medium (Nissui Seiyaku, Co., Japan) supplemented with 2.5% heat-inactivated (56 °C, 30 min) fetal bovine serum (Bioserum, Victoria, Australia), 100 U/ml penicillin, 100 μg/ml streptomycin (GIBCO BRL/Life Technologies, Inc., Gaithersburg, MD) and 12 mmol/l sodium bicarbonate, in humidified atmosphere in 5% CO_2 in air at 37 °C.

2.2. IFN and reagents

IFN-αCon1 (Advaferon®) was kindly provided by Yamanouchi Pharmaceutical Co., Ltd (Tokyo, Japan). Specific activity of the IFN-αCon1 was 1×10^9 IU/mg protein.

A rat antibody against mouse endothelial cells (anti-CD34, clone MEC14.7, Serotec Co., UK), a mouse monoclonal antibody against human alpha-smooth muscle actin (α-SMA) (clone 1A4, Immunon, Pittsburgh, PA) that cross-reacts with mouse α-SMA, Histofine simple stain mouse MAX-PO (Rat) kits (Nichirei, Tokyo, Japan), and HistoMouse™-plus kits (Zymed Laboratories, Inc., CA) were used for immunohistochemical staining.

2.3. Morphological observation

For morphologic observation under a light microscope, cultured cells were seeded on Lab-Tek tissue culture chamber slides (Nunc, Inc., Roskilde, Denmark), cultured with IFN-αCon1 (0.256, 1.024 or 4.096 ng/ml) or without IFN-αCon1 for 72 h, fixed for 10 min in Carnoy's solution, and stained with hematoxylin-eosine (HE).

2.4. Effects of IFN-αCon1 on the proliferation of hepatocellular carcinoma and combined hepatocellular and cholangiocarcinoma cell lines in vitro

The effects of IFN-αCon1 to the growth of cultured cells were examined with colorimetry using 3-(4,5-dimethylthiazol-2yl-yl)-2,5-diphenyl tetrazolium bromide (MTT) assay kits (Chemicon, Temecula, CA) as previously described [13]. Briefly, cells ($1.5–8\times10^3$ cells per well) were seeded on 96-well plates (Falcon, Becton Dickinson Labware, Tokyo, Japan), cultured for 24 h, and the culture medium was changed to a new one with or without IFN-αCon1 (0.004, 0.016, 0.064, 0.256 or 1.024 ng/ml). After the culture for 24, 48, 72 or 96 h, the number of viable cells was examined.

2.5. Quantitative analysis of apoptotic induced by IFN-αCon1 in vitro

Cells cultured with or without 1 ng/ml IFN-αCon1 for 72 h were stained with Annexin V-EGFP (enhanced green fluorescent protein) Apoptosis Detection Kits (Medical and Biological Laboratories Co., Ltd) according to the manufacturer's protocol. After staining, the cells were analyzed using a FACScan (Becton Dickinson Immunocytometry Systems USA), and annexin V-EGFP-positive apoptotic cell rate was determined.

2.6. Effects of IFN-αCon1 on HCC cell proliferation in nude mice

Cultured KIM-1 or HAK-1B (10^7 cells/mouse) was subcutaneously (s.c.) injected to the back of 5-week old female BALB/c athymic nude mice (Clea Japan, Inc., Osaka, Japan). Five to seven days later when the largest diameter of the tumor reached approximately 5–10 mm, the mice were divided into four groups ($n=10$ each) in a manner to equalize the mean tumor diameter of every group. Each mouse received a subcutaneous injection of 0.1 ml of phosphate buffered saline (PBS) containing either 0, 0.01, 0.1 or 1 μg of IFN-αCon1 once a day for 2 weeks. The site of injection was at least 2 cm away from the tumor. During this 2-week period, tumor size was measured in two directions using calipers once in every 2 days and tumor volume (mm^3) was estimated using the equation length$\times$(width)$^2\times0.5$. Tumor volume was estimated on the first day of s.c. injection (Day 0), and then once in every 2 days until Day 14 and the group mean was obtained. On Day 15, the mice were sacrificed and the tumors were resected and fixed in formalin. Tumor sections having the largest diameter were prepared into paraffin sections for HE staining and immunohistochemistry. Every mouse received intraperitoneal injection of 5-bromo-2-deoxyuridine (BrdU) 1 mg (Sigma Chemical Co., St. Louis, MO) 1 h before sacrifice.

The number of cells showing characteristics of apoptosis (e.g. cytoplasmic shrinkage, chromatin condensation, and nuclear fragmentation), was counted in ten 0.25 mm^2-areas within an HE-stained specimen where apoptotic cells were present at a relatively uniform density, and the average number per area was obtained. The TUNEL technique (ApopTag® Peroxidase In Situ apoptosis Detection Kits, CHEMICON International, Inc, CA) was used to detect apoptotic cells. Average number of TUNEL-positive cells per area was obtained, as described above.

KIM-1 tumor sections obtained from every dosage-group were immunostained for incorporated BrdU using BrdU Staining Kits (Oncogene Research Products, Boston, MA), and the average number of positive cells per area was obtained, as described above.

Animals received humane care according to the criteria outlined in the 'Guide for the Care and Use of Laboratory Animals' prepared by the National Academy of Sciences and published by the National Institutes of Health (NIH publication 86-23 revised 1985).

2.7. Immunohistochemistry

For double-immunostaining, tumor sections were reacted with anti-mouse endothelial cell antibody using Histofine simple stain mouse MAX-PO (Rat) kits at first. Peroxidase reaction was developed using the mixture of 3,3-diaminobenzidine tetrahydrochloride (DAB). The second staining with anti-human α-SMA antibody was conducted by making the section react to the primary antibody, α-SMA, at 4 °C overnight, and using HistoMouse™-plus kits. The sections were developed using the mixture of a commercial chromogen (VIP) and hydrogen peroxide (Vector VIP Substrate Kit, Vector Laboratories, CA), and counterstaining was performed using hematoxylin.

The number of blood vessels in the tumor and in the borderline area between the tumor nodule and surrounding tissues was counted on each specimen. The size of the counted area was measured by tracing the outline displayed on a computer-monitor using Cosmozone-1S computer imaging-analysis system (Nikon Co., Tokyo, Japan). From the obtained number of the vessels per unit area (mm^2), the group mean was obtained for group comparison.

2.8. Statistics

Comparison of estimated tumor volume was performed using two-factor factorial ANOVA and Student's *t*-test. The other data-comparisons were performed using Student's *t*-test.

3. Results

3.1. Effects of IFN-αCon1 on liver cancer cell proliferation in vitro

Ten percent or more decrease in the relative viable cell number (Fig. 1A) occurred in all 13 cell lines after 72 h or later after the addition of 1.024 ng/ml (1024 IU/ml) of IFN-αCon1. In KMCH-2, proliferation was suppressed 24 h after the IFN-αCon1 contact, and the cell number reached a plateau afterwards. In KIM-1, HAK-2 and HAK-6, proliferation was suppressed up to 72 h and the cell number reached a plateau afterwards. In the other 9 cell lines, proliferation was suppressed in a varying degree of up to 96 h.

Ninety-six hours after the addition of IFN-αCon1, the relative viable cell number was suppressed in every cell line in a dose-dependent manner (Fig. 1B). The relative cell number of all 13 cell lines when they were cultured for 96 h with 1.024 ng/ml of IFN-αCon1 ranged between 29 and 74%, and their mean was 53±16% (SD). In the 7 cell lines (HAK-6, KYN-1, KMCH-1, KYN-2, KIM-1, HAK-1B, and KYN-3), the number was suppressed to 50% or lower with 1.024 ng/ml of IFN-αCon1, and 50% inhibitory concentration (IC50) was 0.128, 0.204, 0.214, 0.352, 0.612, 0.666, and 0.804 ng/ml, respectively. No relationship was detected between the histologic differentiation level of original tumor and sensitivity to the antiproliferative effect of IFN-αCon1.

Seventy-two hours after adding IFN-αCon1, every cell line showed characteristics of apoptosis, e.g. cytoplasmic shrinkage, chromatin condensation, and nuclear fragmentation, in various degrees and in a dose-dependent manner (Fig. 2).

Quantitative analysis of annexin V-EGFP-positive apoptotic cells revealed that the appearance of apoptosis was significantly higher in the cultures with IFN-αCon1 than those without IFN-αCon1 in all cell lines (Table 1).

3.2. Effects of IFN-αCon1 on HCC cell proliferation in nude mice

Chronological changes of estimated tumor volume after subcutaneous injection of cultured KIM-1 or HAK-1B cells

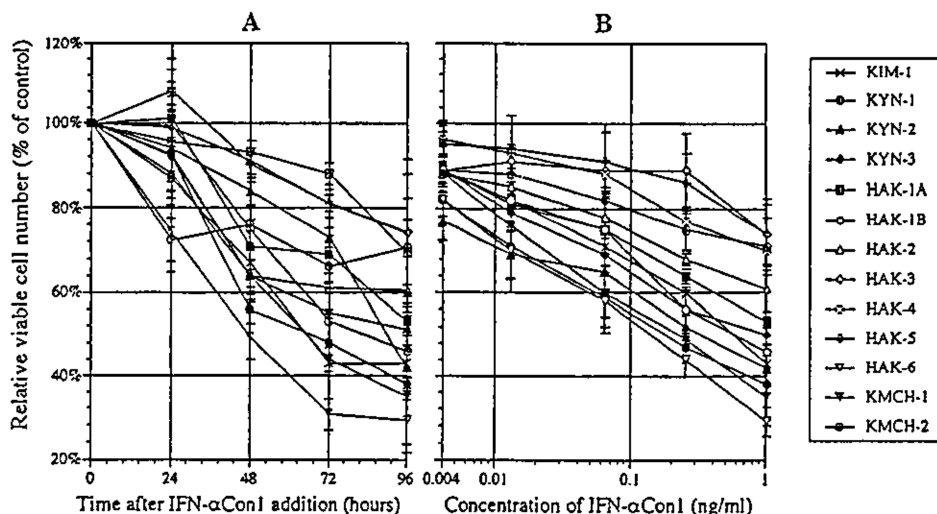

Fig. 1. Antiproliferative effect of IFN-αCon1. (A) Chronological changes in relative viable cell number (% of the control) after adding 1.024 ng/ml (1024 IU/ml) of IFN-αCon1. Growth was suppressed with time. (B) 96 h after adding 0.004, 0.016, 0.064, 0.256 or 1.024 ng/ml of IFN-αCon1. Cell proliferation was suppressed in a dose-dependent manner but in varying degrees. The suppression was statistically significant ($P<0.01$–0.0001) in the range of 4–1.024 ng/ml of IFN-αCon1 in all cell lines. Specific activity of the IFN-αCon1 was 1×10^9 IU/mg protein. Eight samples were used in each experiment ($n=8$). The experiment was repeated at least three times for each cell line to confirm reproducibility of the data, and almost identical results were obtained. Error bar represents SE. Mean absorbance in the control (cells cultured in the medium without IFN-αCon1) was determined as 100%, and the mean of the other groups was expressed as a ratio.

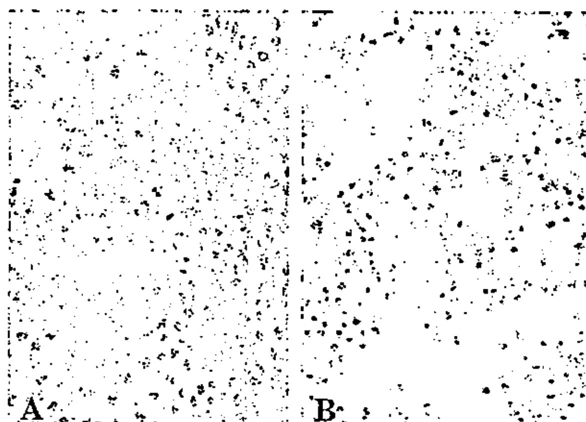

Fig. 2. Photomicrographs of HAK-6 cells cultured for 72 h on a Lab-Tek Chamber slide. (A) No IFN-αCon1 in culture medium. (B) With 1.024 ng/ml (1024 IU/ml) of IFN-αCon1 in culture medium. IFN-αCon1-induced apoptosis was characterized by cytoplasmic shrinkage, chromatin condensation and nuclear fragmentation (HE staining, ×100).

to nude mice are summarized in Fig. 3. Significant difference on the volume changes was obtained between the control and each KIM-1 and HAK-1B tumor group with IFN-αCon1 ($P<0.0001$ by two-factor factorial ANOVA). In KIM-1, tumor volume became significantly smaller than the controls after the 4th day of culture ($P<0.05$–0.0001 by Student t-test) except the 6th day of 0.1 μg (10^5 IU) IFN-αCon1. In HAK-1B, significant difference to the controls was obtained after the 2nd day of 1 μg (10^6 IU), the 6th day of 0.1 μg and the 10th day of 0.01 μg (10^4 IU) ($P<0.05$–0.0001 by Student t-test). Except for the initial 8 days of the KIM-1 group, tumor volumes of both KIM-1

Table 1
Quantitative analysis of apoptosis induced by IFN-αCon1 in 13 liver cancer cell lines

Cell line	Annexin V-EGFP-positive apoptotic cell rates (%)	
	Control	IFN-αCon1
KIM-1	6.0±0.8	22.1±1.3[a]
KYN-1	10.6±1.0	16.9±2.6[b]
KYN-2	11.7±3.2	34.9±4.3[a]
KYN-3	6.0±0.7	15.2±0.9[a]
HAK-1A	10.7±1.7	20.3±1.2[a]
HAK-1B	8.0±1.4	28.7±0.8[a]
HAK-2	6.1±2.0	15.7±0.9[a]
HAK-3	6.4±0.7	9.1±0.8[b]
HAK-4	3.3±0.4	5.0±0.5[b]
HAK-5	7.3±1.2	10.8±1.3[c]
HAK-6	9.1±1.5	20.1±0.9[a]
KMCH-1	5.2±0.4	27.1±1.3[a]
KMCH-2	4.0±0.5	5.1±0.8*

Cells were cultured with medium alone (control) or medium with 1 ng/ml (1000 IU/ml) IFN-αCon1. Apoptosis was measured by Annexin V-EGFP staining. Annexin V-EGFP-positive apoptotic cell rates are given as average±SD. Five samples were used in each experiment. *$P<0.05$ vs. corresponding control value.

[a] $P\leq0.0001$ vs. corresponding control value.

[b] $P\leq0.001$ vs. corresponding control value.

[c] $P<0.01$ vs. corresponding control value.

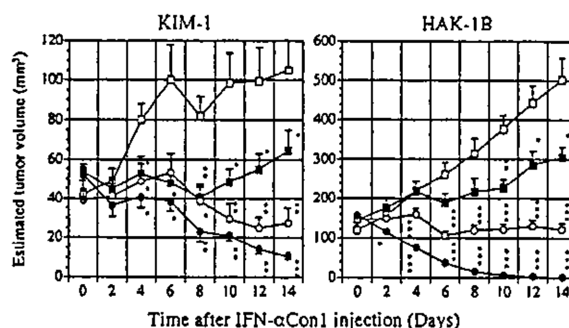

Fig. 3. Time-course change of estimated tumor volumes of subcutaneous human HCC tumors (KIM-1 and HAK-1B cells) in nude mice. Mice received subcutaneous injection of 0.01 μg (10^4 IU) IFN-αCon1 (■), 0.1 μg (10^5 IU) IFN-αCon1 (O), or 1 μg (10^6 IU) IFN-αCon1 (●), or PBS alone (control) (□). In mice with HAK-1B, tumor became almost unrecognizable on Day10. *$P<0.05$, vs. control. **$P<0.005$, vs. control. ***$P<0.0001$, vs. control (by Student t-test).

and HAK-1B were suppressed dose-dependently. At the end of this experiment, estimated volumes in the KIM-1 and HAK-1B groups that received 0.01 μg (10^4 IU) of IFN-αCon1 (4×10^5 IU/kg, the closest to the clinical dosage 3×10^5 IU/kg) became 62 and 61%, respectively, of the control. In the mice that received 0.1 μg, the volumes became 26 and 24%, respectively, of the control. In the mice that received 1 μg, the volume shrunk to 10% of the control in the KIM-1 group and almost disappeared on the 10th day in the HAK-1B group (Fig. 4). IFN-αCon1 administration did not affect mouse body weight (data not shown).

Fig. 4. A photograph of a control group nude mouse (right side) and a 1 μg IFN-αCon1 group nude mouse (left side) on day 15. The control group mouse has a distinct large subcutaneous tumor (right side), while the 1 μg IFN-αCon1 group mouse has no visible subcutaneous tumor (left side).

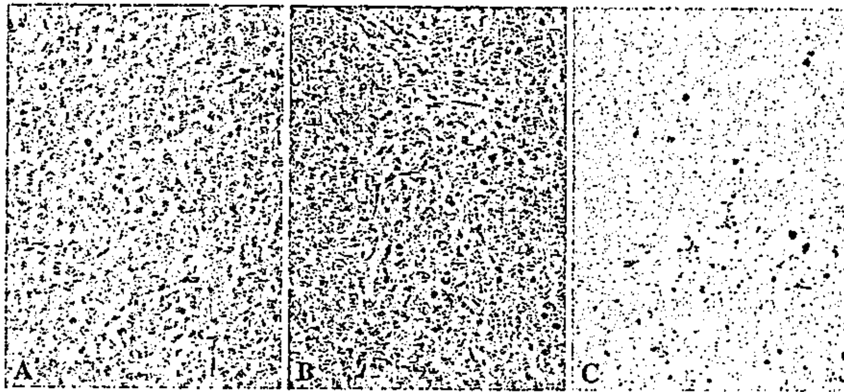

Fig. 5. Photomicrograph of subcutaneous human HCC tumors developed after injection of HAK-1B cells in nude mice. (A) A control mouse that received PBS alone. Thick trabecular or compact arrangement of tumor cells is noted. (B) A mouse that received s.c. injection of 0.1 μg (10^5 IU) IFN-αCon1. There are many apoptotic tumor-cells characterized by shrinkage and/or eosinophilic change in cytoplasm, and by chromatin condensation and/or fragmentation of nuclei (HE staining, ×200). (C) The same tumor as shown in (B). There are many TUNEL-positive cells showing brown nuclei (stained by the TUNEL technique).

Histological examination on KIM-1 and HAK-1B tumor specimens stained with HE revealed that the numbers of apoptotic cells in the groups treated with IFN-αCon1 were significantly higher than that of the control and increased dose-dependently. The incidence of apoptosis in TUNEL-stained sections showed the same tendencies as those obtained in HE-stained sections (Fig. 5 and Table 2). Tissues on the site of tumor that disappeared in the 1 μg group presented only mild increase in fibroblasts.

The number of blood vessels per unit area in the nude mice that received injection of either KIM-1 or HAK-1B was different in every group, and the number tended to decrease dose-dependently. Significant difference was obtained between the control and 1 μg in the KIM-1 group, and between the control and 0.1 μg or 0.01 μg in the HAK-1B group (Figs. 6 and 7).

Table 2
Comparison of apoptotic cell number in the subcutaneous tumors in nude mice

Group	Apoptotic cell number	
	HE stain	TUNEL method
KIM-1 tumor		
Control	8.4±0.8	4.1±1.3
0.01 μg (10^4 IU) IFN-αCon1	13.2±1.4[a]	6.0±0.8
0.1 μg (10^5 IU) IFN-αCon1	17.6±0.9[b]	16.5±3.7[a]
1 μg (10^6 IU) IFN-αCon1	28.2±1.2[b]	20.5±5.1[*]
HAK-1B tumor		
Control	12.0±0.9	5.3±1.2
0.01 μg (10^4 IU) IFN-αCon1	15.9±1.0[a]	9.8±1.8
0.1 μg (10^5 IU) IFN-αCon1	19.2±0.6[b]	13.5±2.2[*]

Results are given as average±SE. The number of cells showing morphological characteristics of apoptosis (e.g. cytoplasmic shrinkage, chromatin condensation, and nuclear fragmentation), was counted in ten 0.25 mm^2-areas within a HE-stained specimen. The number of TUNEL-positsive cells was also counted in the same manner. All subcutaneous tumors disappeared in the nude mice that received s.c. injection of 1 μg IFN-αCon1. [*] $P<0.05$ vs. corresponding control value.

[a] $P<0.01$ vs. corresponding control value.

[b] $P\leq 0.0001$ vs. corresponding control value.

Immunohistochemical examination of BrdU uptake of KIM-1 tumors revealed that BrdU-positive cells were present mainly on the edge of the tumor nodules in every dosage-group, but there was no group difference in the positive rate.

4. Discussion

The addition of IFN-αCon1 to culture medium induced dose-dependent and time-dependent antiproliferative effects in most of the 13 cell lines, and a certain degree of apoptosis in all 13 cell lines. There was no relationship between the histological level and the sensitivity to IFN-αCon1. Although in vitro antiproliferative findings may not be exactly the same in clinical applications, these findings indicate that IFN-αCon1 may be efficacious in treatments of HCC at various histological levels and types.

In our animal experiment, estimated tumor volume decreased dose-dependently with the subcutaneous

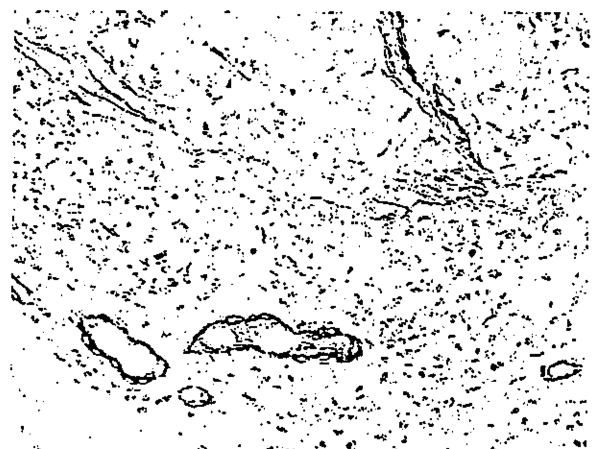

Fig. 6. Photomicrograph showing double immunostained artery-like blood vessels in a subcutaneous human HCC tumor developed after the injection of HAK-1B cells in nude mice.

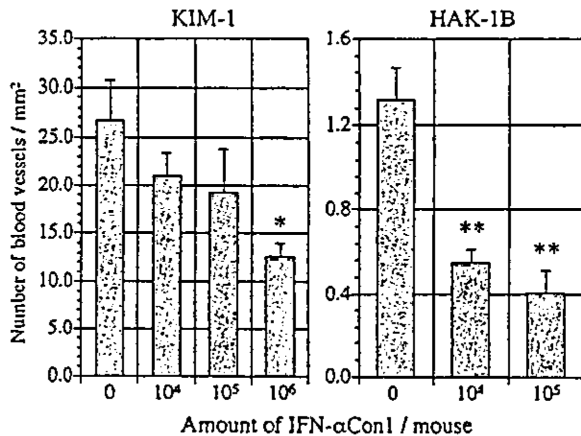

Fig. 7. Comparison of blood vessel number of the subcutaneous tumors in nude mice that received s.c. injection of 0.01 μg (10^4 IU), 0.1 μg (10^5 IU) or 1 μg (10^6 IU) IFN-αCon1 or PBS alone every day for consecutive 14 days. Number of artery-like blood vessel in and around tumor decreased in a dose-dependent manner. Subcutaneous HAK-1B tumors disappeared in all nude mice that received s.c. injection of 1 μg (10^6 IU) IFN-αCon1. The error bar represents SE. *$P<0.05$ vs. control. **$P<0.003$ vs. control.

injection of 0.01–1 μg (10^4–10^6 IU) of IFN-αCon1 per mouse. In mice that received any of the doses apart from the 0.01 μg dose, tumor volume decreased over time, and the tumor completely disappeared in the HAK-1B group with 1 μg. In the histological examination of the tumor in mice with IFN-αCon1 treatment, apoptotic cells appeared more frequently in a dose-dependent manner. Another well-known growth inhibitory mechanism induced by IFN-α is the induction of blockage of cell-cycle progression at G1, S, or G_2/M [21–26]. BrdU uptake of KIM-1 tumors was examined in every dosage-group, but there was no significant group difference in the positive rate. This finding however does not agree with our previous conclusion, i.e. natural human IFN-α arrests cell growth at the S phase and this increases BrdU-positive cells in the 2 cell lines [13]. This difference is probably attributable to the difference of in vitro and in vivo experiments. Our previous conclusion was derived from an in vitro experiment over a short culture period (96 h), while the current study examined tumor cells in vivo after a 2-week administration period. In this in vivo experiment, apoptosis holds the dominant position over the arrest of the cell cycle and this results in growth suppression. Further studies, including measurement of the cell-cycle-related protein (e.g. cyclins and cyclin-dependent kinases) levels in nude mouse tumors are planned.

The number of blood vessels per unit area decreased dose-dependently in KIM-1 and HAK-1B nodules. IFN suppresses angiogenesis within the nodules of human bladder carcinoma and human malignant glioma [38,39], and the current study demonstrates that IFN-αCon1 suppresses angiogenesis in HCC nodules. Dinney et al. [38] reported the possible involvement of basic fibroblast growth factor (bFGF) in the suppressive effect of IFN for angiogenesis. On the other hand, Hong et al. [39] found no relationship between the suppression of angiogenesis due to IFN and the expression of bFGF or vascular endothelial growth factor (VEGF). Investigations on the expression of angiogenesis factors (e.g. bFGF, VEGF, and IL-8) in HCC tumors in nude mice treated or untreated with IFN-αCon1 provide useful information and are now underway.

Clinical trials of IFN-α in treatment for HCC did not achieve consistent results. One study using very high doses of IFN (from 25 to 50×10^6 IU of recombinant IFN-α2a) showed beneficial effects [40], whereas other studies using low doses (less than 15×10^6 IU) did not show significant antitumor effects [41–43]. Although these findings suggest the efficacy of high-dose IFN-α treatment on progressed HCC, high-dose administration of conventional IFN-α often causes side effects and patients may develop intolerable conditions and withdraw from the treatment. In regards to side effects, IFN-αCon1 at the same mass concentration of conventional IFN-α is expected to have higher antiviral and antitumor activities because of its higher specific activity, and IFN-αCon1 at a usual clinical dose possibly suppresses the growth of HCC. In chronic hepatitis C patients who received subcutaneous injection of IFN-αCon1 at a clinical dose (18×10^6 IU) for 14 consecutive days, the maximum serum level of IFN-αCon1 reached 372 IU/ml (unpublished data). This level was higher than the IC50 in the four cell lines (0.128–0.352 ng/ml (128–352 IU/ml)[KYN-1, KYN-2, HAK-6 and KMCH-1]) 96 h after the addition of IFN-αCon1 to culture medium. In the current animal experiment, a dose similar to the clinical dose used in treatment for HCV-related chronic hepatitis suppressed HCC growth in nude mice. These data indicate the potential clinical application of IFN-αCon1 in the prevention and treatment of HCC.

Anti-oncogenic properties of IFN-α during the preneoplastic steps have been studied in animal models. In a 2-phase model of rat hepatocarcinogenesis, preneoplastic hepatocytes in rats that received IFN-α2b during the initiation stage were shown to undergo programmed cell death [46]. However, the study in *X/myc* transgenic mouse showed that IFN-α did not affect hepatocyte apoptosis or telomerase activity at early premalignant stages, but did downregulate hepatocyte proliferation and *c-myc* over-expression at these steps, leading to a delay of HCC onset and increase of overall survival [44,45]. This result at least suggests that the antioncogenic effect of IFN-α is probably diverse. We speculate that IFN-αCon1 administered to chronic viral hepatitis patients would inhibit the growth of clinically undetectable HCC by directly inducing apoptosis of HCC cells and by indirectly suppressing tumor angiogenesis and prevent or delay the development of HCC in these patients.

Acknowledgements

We thank Ms Akemi Yamashita and Ms Kayoko Najima for their assistance in our experiments, and Dr Hiroki

Inutsuka of Office of Medical Education, Kurume University for his assistance in statistical analysis. This study was supported in part by the Sarah Cousins Memorial Fund, Boston, Massachusetts, and by a Grant-in-Aid for Scientific Research (C) from the Ministry of Education, Science, Sports and Culture, Japan (No. 13670233).

References

[1] Bréchot C, Jaffredo F, Lagorce D, Gerken G, Büchenfelde KM, Papakonstoninou A, et al. Impact of HBV, HCV and GBV-C/HGV on hepatocellular carcinoma in Europe: results of a European concerted action. J Hepatol 1998;29:173–183.
[2] Di Bisceglie AM, Order SE, Klein JL, Waggoner JG, Sjogren MH, Kuo G, et al. The role of chronic viral hepatitis in hepatocellular carcinoma in the United States. Am J Gastroenterol 1991;86:335–338.
[3] Shiratori Y, Shiina S, Imamura M, Kato N, Kanai F, Okudaira T, et al. Characteristic difference of hepatocellular carcinoma between hepatitis B- and C-viral infection in Japan. Hepatology 1995;22: 1027–1033.
[4] Gutterman JU. Cytokine therapeutics: Lessons from interferon-α. Proc Natl Acad Sci USA 1994;91:1198–1205.
[5] Ikeda K, Saitoh S, Arase Y, Chayama K, Suzuki Y, Kobayashi M, et al. Effect of interferon therapy on hepatocellular carcinogenesis in patients with chronic hepatitis type C: A long-term observation study of 1,643 patients using statistical bias correction with proportional hazard analysis. Hepatology 1999;29:1124–1130.
[6] Mazzella G, Accogli E, Sottili S, Festi D, Orsini M, Salzetta A, et al. Alpha interferon treatment may prevent hepatocellular carcinoma in HCV-related liver cirrhosis. J Hepatol 1996;24:141–147.
[7] Nishiguchi S, Kuroki T, Nakatani S, Morimoto H, Takeda T, Nakajima S, et al. Randomised trial of effects of interferon-α on incidence of hepatocellular carcinoma in chronic active hepatitis C with cirrhosis. Lancet 1995;346:1051–1055.
[8] Stark GR, Kerr IM, Williams BR, Silverman RH, Schreiber RD. How cells respond to interferons. Annu Rev Biochem 1998;67: 227–264.
[9] Xu D, Erickson S, Szeps M, Gruber A, Sangfelt O, Einhorn S, et al. Interferon α down-regulates relomerase reverse transcriptase and telomerase activity in human malignant and nonmalignant hempatopoietic cells. Blood 2000;96:4313–4318.
[10] Negrier S, Escudier B, Lasset C, Douillard JY, Savary J, Chevreau C, et al. Recombinant human interleukin-2, recombinant human interferon alfa-2a, or both in metastatic renal-cell carcinoma. Groupe Francais d'Immunotherapie. N Engl J Med 1998;338:1272–1278.
[11] Huber BE, Wirth PJ, Newbold JE. Effects of human lymphoblastoid interferon on proliferation, gene expression and tumourigenicity of human hepatoma cell lines. Drugs Exp Clin Res 1991; 17:281–291.
[12] Dunk AA, Ikeda T, Pignatelli M, Thomas HC. Human lymphoblastoid interferon: in vitro and in vivo studies in hepatocellular carcinoma. J Hepatol 1986;2:419–429.
[13] Yano H, Iemura A, Haramaki M, Ogasawara S, Takayama A, Akiba J, et al. Interferon alfa receptor expression and growth inhibition by interferon alfa in human liver cancer cell lines. Hepatology 1999;29: 1708–1717.
[14] Murphy D, Detjen KM, Welzel M, Wiedenmann B, Rosewicz S. Interferon-alpha delays S-phase progression in human hepatocellular carcinoma cells via inhibition of specific cyclin-dependent kinases. Hepatology 2001;33:346–356.
[15] Milner AE, Grand RJ, Gregory CD. Effects of interferon-alpha on human B cells: Repression of apoptosis and prevention of cell growth are independent responses of Burkitt lymphoma lines. Int J Cancer 1995;61:348–354.
[16] Torcia M, Lucibello M, De Chiara G, Labardi D, Nencioni L, Bonini P, et al. Interferon-alpha-induced inhibition of B16 melanoma cell proliferation: interference with the bFGF autocrine growth circuit. Biochem Biophys Res Commun 1999;262:838–844.
[17] Thulasi R, Dias P, Houghton PJ, Houghton JA. Alpha 2a-interferon-induced differentiation of human alveolar rhabdomyosarcoma cells: correlation with down-regulation of the insulin-like growth factor type I receptor. Cell Growth Differ 1996;7:531–541.
[18] Sangfelt O, Erickson S, Castro J, Heiden T, Einhorn S, Grandér D. Induction of apoptosis and inhibition of cell growth are independent responses to interferon-α in hematopoietic cell lines. Cell Growth Differ 1997;8:343–352.
[19] Rodríuez-Villanueva J, MacDonnell TJ. Induction of apoptotic cell death in non-melanoma skin cancer by interferon-α. Int J Cancer 1995;61:110–114.
[20] Selleri C, Sato T, Vecchio LD, Luciano L, Barrett AJ, Rotoli B, et al. Involvement of Fas-mediated apoptosis in the inhibitory effects of interferon-α in chronic myelogenous leukemia. Blood 1997;89: 957–964.
[21] Melamed D, Tiefenbrun N, Yarden A, Kimchi A. Interferons and interleukin-6 suppress the DNA-binding activity of E2F in growth-sensitive hematopoietic cells. Mol Cell Biol 1993;13: 5255–5265.
[22] Creasey AA, Bartholomew JC, Merigan TC. Role of G_0-G_1 arrest in the inhibition of tumor cell growth by interferon. Proc Natl Acad Sci USA 1980;77:1471–1475.
[23] Roos G, Leanderson T, Lundgren E. Interferon-induced cell cycle changes in human hematopoietic cell lines and fresh leukemic cells. Cancer Res 1984;44:2358–2362.
[24] Numa Y, Kawamoto K, Sakai N, Matsumura H. Flow cytometric analysis of antineoplastic effects of interferon-α, β and γ labelled with fluorescein isothiocyanate on cultured brain tumors. J Neuro-Oncol 1991;11:225–234.
[25] Nikolaeva TG, Timofeev IV, Dobrynin IaV. Effect of interferon on cell cycle phases in cultured human tumor cells. Eksp Onkol 1984;6: 52–55.
[26] Mandal M, Bandyopadhyay D, Goepfert TM, Kumar R. Interferon-induces expression of cyclin-dependent kinase-inhibitors $p21^{WAF1}$ and $p27^{Kip1}$ that prevent activation of cyclin-dependent kinase by CDK-activating kinase (CAK). Oncogene 1998;16:217–225.
[27] Blatt LM, Davis JM, Klein SB, Taylor MW. The biologic activity and molecular characterization of a novel synthetic interferon-alpha species, consensus interferon. J Interferon Cytokine Res 1996;16: 489–499.
[28] Ozes ON, Reiter Z, Klein S, Blatt LM, Taylor MW. A comparison of interferon-Con1 with natural recombinant interferons-alpha: antiviral, antiproliferative, and natural killer-inducing activities. J Interferon Res 1992;12:55–59.
[29] Klein SB, Blatt LM, Taylor MW. Cell surface binding characteristics correlate with consensus type I interferon enhanced activity. J Interferon Cytokine Res 1996;16:1–6.
[30] Murakami T. Establishment and characterization of human hepatoma cell line (KIM-1). Acta Hepatol Jpn 1984;25:532–539.
[31] Yano H, Kojiro M, Nakashima T. A new human hepatocellular carcinoma cell line (KYN-1) with a transformation to adenocarcinoma. In Vitro Cell Dev Biol 1986;22:637–646.
[32] Yano H, Maruiwa M, Murakami T, Fukuda K, Ito Y, Sugihara S, et al. A new human pleomorphic hepatocellular carcinoma cell line, KYN-2. Acta Pathol Jpn 1988;38:953–966.
[33] Murakami T, Maruiwa M, Fukuda K, Kojiro M, Tanaka M, Tanikawa K. Characterization of a new human hepatoma cell line (KYN-3) derived from the ascites of the hepatoma patient [Abstract]. Jpn J Cancer Res 1988;292. Proceedings of the Japanese Cancer Association.
[34] Yano H, Iemura A, Fukuda K, Mizoguchi A, Haramaki M, Kojiro M. Establishment of two distinct human hepatocellular carcinoma cell

lines from a single nodule showing clonal dedifferentiation of cancer cells. Hepatology 1993;18:320–327.

[35] Haramaki M, Yano H, Iemura A, Momosaki S, Ogasawara S, Inoue M, et al. A new human hepatocellular carcinoma cell line (HAK-2) forms various structures in collagen gel matrices. Hum Cell 1997;10:183–192.

[36] Murakami T, Yano H, Maruiwa M, Sugihara S, Kojiro M. Establishment and characterization of a human combined hepatocholangiocarcinoma cell line and its heterologous transplantation in nude mice. Hepatology 1987;7:551–556.

[37] Yano H, Iemura A, Haramaki M, Momosaki S, Ogasawara S, Higaki K, et al. A human combined hepatocellular and cholangiocarcinoma cell line (KMCH-2) that shows the features of hepatocellular carcinoma or cholangiocarcinoma under different growth conditions. J Hepatol 1996;24:413–422.

[38] Dinney CP, Bielenberg DR, Perrotte P, Reich R, Eve BY, Bucana CD, et al. Inhibition of basic fibroblast growth factor expression, angiogenesis, and growth of human bladder carcinoma in mice by systemic interferon-alpha administration. Cancer Res 1998;58: 808–814.

[39] Hong YK, Chung DS, Joe YA, Yang YJ, Kim KM, Park YS, et al. Efficient inhibition of in vivo human malignant glioma growth and angiogenesis by interferon-beta treatment at early stage of tumor development. Clin Cancer Res 2000;6:3354–3360.

[40] Lai CL, Lau JYN, Wu P, Ngan H, Chung HT, Mitchell SJ, et al. Recombinant interferon-α in inoperable hepatocellular carcinoma: a randomized controlled trial. Hepatology 1993;17:389–394.

[41] Sachs E, Di Bisceglie AM, Dusheiko GM, Song E, Lyons SF, Schoub BD, et al. Treatment of hepatocellular carcinoma with recombinant leucocyte interferon: a pilot study. Br J Cancer 1985;52: 105–109.

[42] The Gastrointestinal Tumor Study Group. A prospective trial of recombinant human interferon alpha 2B in previously untreated patients with hepatocellular carcinoma. Cancer 1990;66:135–139.

[43] Llovet JM, Sala M, Castells L, Suarez Y, Vilana R, Bianchi L, Ayuso C, et al. Randomized controlled trial of interferon treatment for advanced hepatocellular carcinoma. Hepatology 2000;31:54–58.

[44] Merle P, Barraud L, Lefrançois L, Chevallier M, Guerret S, Maisonnas M, et al. Lont-term high-dose interferon-α therapy delays Hepadnavirus-related hepatocarcinogenesis in X/myc transgenic mice. Oncogene 2003;22:2762–2771.

[45] Merle P, Chevallier M, Levy R, Maisonnas M, Terradillos O, Si Ahmed S, et al. Preliminary results of interferon-α therapy on woodchuck hepatitis virus-induced hepatocarcinogenesis: possible benefit in female transgenic mice. J Hepatol 2001;34:562–569.

[46] Alvarez M, Cerliani J, Monti J, Carnovale C, Ronco M, Pisani G, et al. The in vivo apoptotic effect of interferon alfa-2b on rat preneoplastic liver involves bax protein. Hepatology 2002;35:824–833.

Reprinted by

ELSEVIER

Contact: Elizabeth Drayton
Tel: +44 (0) 1865 843548
Fax: +44 (0) 1865 843976
Email: e.drayton@elsevier.com
http://intl.elsevierhealth.com/journals

特別講演-1

IFNの肝癌細胞に対する直接的な増殖抑制作用

久留米大学医学部病理学教室助教授　矢野 博久

はじめに

インターフェロンα(interferonα：IFNα)は，抗ウイルス作用，細胞増殖抑制作用，免疫応答調節作用など，多彩な生物活性を有するサイトカインである[1]。臨床的には，抗ウイルス薬としてC型慢性肝炎に，抗腫瘍薬として慢性骨髄性白血病や腎細胞癌などの治療に使用されている[2]。

C型慢性肝炎は，長期的経過で肝硬変・肝細胞癌へと進展する例が多く，肝病変の進展阻止は重要な問題である。C型慢性肝炎あるいは肝硬変に対してIFN療法を行うと，ウイルスの完全排除の有無にかかわらず有意に肝発癌率が低下すると，複数の施設から報告されている[3,4]。さらに，最近では肝細胞癌の切除術後の再発防止にIFN投与が有効であるという報告[5,6]や，IFN抗癌薬の併用療法が進行肝癌の治療に有用であるという報告もある[7,8]。肝癌発生予防や治療に対するIFNの有用性が臨床的に明らかにされつつあるが，その作用メカニズムはいまだ明らかにされていない。IFNαが腫瘍細胞に対する直接的な増殖抑制作用を有することから，肝癌細胞に対しても直接的に発癌抑制や抗癌作用を示している可能性も考えられる。

筆者らは，IFNαの肝癌細胞に対する作用を明らかにするために，IFNαのレセプターの発現，IFNαの増殖抑制作用やその機序解明などに関して，11種類の分化度の異なる肝細胞癌細胞株と2種類の混合型肝癌株の合計13株の肝癌の細胞株を使用して検討を行っているが[9,10]，本稿では，そのデータの一部を紹介する。

肝癌におけるI型IFNレセプターの発現

IFNαの作用発現にはそのレセプターであるI型IFNレセプターの発現が必須である。I型IFNレセプターは，AR-1鎖とAR-2鎖の2つから構成されており，AR-2鎖には，AR-2a，-2b，-2cの3種類があるが，AR-2cが，インターフェロンとの結合ユニットでありIFNの作用発現には最も重要といわれている。AR-1鎖は，高親和性のレセプターを形成するために必要なユニットであるといわれている[1,11,12]。RT-PCR法を用いてmRNAレベルのAR-1鎖とAR-2c鎖の発現を検討したところ，すべての細胞株で発現が確認された。細胞表面のAR-2鎖の発現を蛋白レベルで検討すると13株中12株で発現が確認された。さらに，69例の手術切除肝癌およびその非癌部組織におけるAR-2鎖の発現に関しても免疫組織化学的に検討を行った。その結果，癌部では69例中53例(77 %)に，非癌部では61例(88 %)に陽性所見が認められた。肝細胞癌の分化度・被膜浸潤・肝内転移などの病理学的なパラメーターとAR-2鎖の発現との間に関連性は認めず，非癌部に関しても慢性肝炎と肝硬変で発現の差を認めなかった。このように，肝癌細胞では比較的高頻度にIFNのレセプターを発現していることが明らかとなった。

IFNαの肝癌細胞株に対する増殖抑制作用

ヒト天然型IFNα(1-1024 U/mL，OIF®，大塚製薬株式会社)を13種類の肝癌細胞株の培地に添加し24～96時間培養すると，大部分の細胞株で時間依存性の細胞増殖抑制作用が認められた。また，IFNα接触後96時間目では，すべての細胞

株で種々の程度に濃度依存性に細胞増殖が抑制された。13株中5株では，IFNα接触後96時間目で非添加のコントロールと比べ生細胞数が50%以下まで低下し，これらの細胞株の50%増殖抑制濃度は，86.3 U/mLから465.5 U/mLの範囲内であった。IFNαの増殖抑制作用に対する感受性と細胞株のオリジナル腫瘍の組織学的異型度との間に関連性は認めなかった。また，細胞表面のAR-2鎖の発現は，IFNαによる増殖抑制作用と必ずしも相関していなかった。

IFNαの増殖抑制のメカニズム

IFNαによる細胞増殖抑制のメカニズムを検討するために，IFNαを肝癌細胞の培地に添加し，72時間培養して細胞形態を観察すると細胞質の縮小や核の濃縮・核の断片化など，アポトーシスに特徴的な細胞像の出現が認められた。また，このような細胞からDNAを採取しアガロースゲル内で電気泳動すると，アポトーシスの生化学的なマーカーであるDNA ladderの形成が認められた(図1)。このようなアポトーシスの誘導は，細胞間で程度の差を認めるものの13株中10株で認められた。IFNαによるアポトーシスの誘導時には，cytochrome cのミトコンドリアから細胞質への放出，caspase-9やcaspase-3の活性化が認められることから，ミトコンドリア系を介したアポトーシス誘導経路の関与が推察される(未発表データ)。

また，アポトーシス誘導が認められなかった3株でもIFNαにより細胞数の低下を認め，アポトーシス誘導以外の増殖抑制の機序が存在することが示唆された。そこで次に，IFNαの細胞周期に及ぼす作用の検討を行った。その結果，IFNαによる13の肝癌細胞株の増殖抑制機序として，①アポトーシスの誘導を伴うS期での細胞周期進行停止誘導(9株)，②アポトーシスの誘導を伴わないS期での細胞周期進行停止誘導(2株)，③アポトーシスの誘導を伴うG_2/M期での細胞周期進行停止誘導(1株)，④アポトーシスの誘導を伴わないG_1期での細胞周期進行停止誘導(1株)の4つのパターンが確認された。

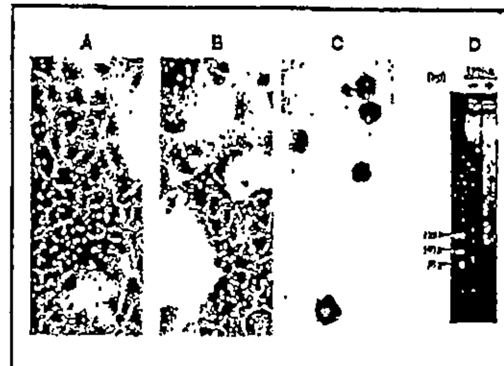

図1　IFNαの肝癌細胞株に対するアポトーシス誘導
A-C：IFNα添加あるいは非添加培養時の肝細胞癌細胞株KIM-1株の細胞形態を示す(A：IFNα非添加培養，200倍。B：IFNα [1000 U/mL OIF®] 添加培養，200倍。C：Bの強拡大，400倍。いずれもヘマトキシリン・エオジン染色)。
D：IFNα添加によりアポトーシスの生化学的指標であるDNAラダーの出現を認める。

IFNαのヌードマウス移植ヒト肝癌に対する抗腫瘍作用

ヌードマウスの皮下に肝細胞癌株(KIM-1あるいはHAK-1B)を移植し，5〜10 mmの腫瘍が出現した時点から14日間連続でコンセンサスIFNであるIFNαCon1 (Advaferon®，山之内製薬株式会社)あるいはPBSのみ(control)を毎日皮下接種し，腫瘍体積の変化をモニターした。マウス1匹に対するIFNαCon1の1日投与量は，0.01，0.1，1 μgとし，最小量(0.01 μg)は，C型慢性肝炎患者への1日の投薬量の1.3倍量にほぼ相当する。その結果，IFNαCon1投与群では，コントロール群と比べ体積が徐々に減少し，15日目では2株とも0.01 μgで60%前後，0.1 μgで25%前後の大きさまで縮小し，1 μgでは，KIM-1は，約10%に，HAK-1Bでは，腫瘍が消失した。皮下腫瘍を組織学的に観察すると，2つの細胞株ともにIFNαCon1投与により濃度依存性に有意に肝癌細胞のアポトーシス数が増加し，さらに腫瘍内の血管数が，減少する傾向を認めた(投稿中)。C型慢性肝炎患者への投薬量でも，肝癌の発育が抑制されたことはIFNが直接的に発癌を抑制する可能性を示唆している。

おわりに

今回の検討により，肝癌細胞がIFNαの作用発現に重要なI型IFNのレセプターのAR-2鎖を発現していることや，IFNαが，肝癌細胞株に対してアポトーシスや細胞周期の進行停止などを誘導し，直接的に増殖を抑制することが示された。前述したように，IFNα投与による肝発癌抑制のメカニズムは，いまだ詳細は解明されていないが，今回のわれわれの検討結果は，IFN投与が直接的に肝発癌を抑制している可能性を支持している。すなわち，IFN投与は，前癌病変あるいは微小な早期肝癌に対して直接的に増殖抑制作用を示し，臨床的な肝癌への進展を遅延あるいは阻止しているのかもしれない。

References

1) Pestka S, Langer JA, Zoon KC, et al：Interferons and their actions. Ann Rev Biochem 56：727-777, 1987
2) Gutterman JU：Cytokine therapeutics：lessons from interferon α. Proc Natl Acad Sci USA 91：1198-1205, 1994
3) Mazzella G, Accogli E, Sottili S, et al：Alpha interferon treatment may prevent hepatocellular carcinoma in HCV-related liver cirrhosis. J Hepatol 24：141-147, 1996
4) Nishiguchi S, Kuroki T, Nakatani S, et al：Randomised trial of effects of interferon-α on incidence of hepatocellular carcinoma in chronic active hepatitis C with cirrhosis. Lancet 346：1051-1055, 1995
5) Ikeda K, Arase Y, Saitoh S, et al：Interferon beta prevents recurrence of hepatocellular carcinoma after complete resection or ablation of the primary tumor-A prospective randomized study of hepatitis C virus-related liver cancer. Hepatology 32：228-232, 2000
6) Kubo S, Nishiguchi S, Hirohashi K, et al：Effects of long-term postoperative interferon-alpha therapy on intrahepatic recurrence after resection of hepatitis C virus-related hepatocellular carcinoma. A randomized, controlled trial. Ann Intern Med 134：963-967, 2001
7) Sakon M, Nagano H, Dono K, et al：Combined intraarterial 5-fluorouracil and subcutaneous interferon-alpha therapy for advanced hepatocellular carcinoma with tumor thrombi in the major portal branches. Cancer 94：435-442, 2002
8) Miyamoto A, Umeshita K, Sakon M, et al：Advanced hepatocellular carcinoma with distant metastases, successfully treated by a combination therapy of alpha-interferon and oral tegafur/uracil. J Gastroenterol Hepatol 15：1447-1451, 2000
9) Takayama A, Yano H, Ogasawara S, et al：Expression of Hu-IFN-α R 2 chain of Type I interferon receptor in human hepatocellular carcinoma and non-cancerous tissues. Int J Mol Med 6：621-627, 2000
10) Yano H, Iemura A, Haramaki M, et al：Interferon alfa receptor expression and growth inhibition by interferon alfa in human liver cancer cell lines. Hepatology 29：1708-1717, 1999
11) Domanski P, Witte M, Kellum M, et al：Cloning and expression of a long form of the b subunit of the interferon αβ receptor that is required for signaling. J Biol Chem 270：21606-21611, 1995
12) Lutfalla G, Holland SJ, Cinato E, et al：Mutant U5A cells are complemented by an interferon-αβ receptor subunit generated by alternative processing of a new member of a cytokine receptor gene cluster. EMBO J 14：5100-5108, 1995